ELM 10552

REPORT DOCUMENTATION PAGE

Form Approved OMB No. 0704-0188

1. REPORT DATE *(DD-MM-YYYY)*	2. REPORT TYPE	3. DATES COVERED *(From – To)*
14-09-2009	Final Report	15 October 2008 - 09-Jun-10

4. TITLE AND SUBTITLE

Design, Manufacturing and Testing of Dual-Layer Frequency-Selective Subwavelength-Grid Polarizers of Enhanced Performance in THz Band

5a. CONTRACT NUMBER
FA8655-08-1-3049

5b. GRANT NUMBER

5c. PROGRAM ELEMENT NUMBER

6. AUTHOR(S)

Dr. Vladimir B Yurchenko

5d. PROJECT NUMBER

5d. TASK NUMBER

5e. WORK UNIT NUMBER

7. PERFORMING ORGANIZATION NAME(S) AND ADDRESS(ES)

National University of Ireland Maynooth
Main St.
Maynooth 00000
Republic of Ireland

8. PERFORMING ORGANIZATION REPORT NUMBER

N/A

9. SPONSORING/MONITORING AGENCY NAME(S) AND ADDRESS(ES)

EOARD
Unit 4515 BOX 14
APO AE 09421

10. SPONSOR/MONITOR'S ACRONYM(S)

11. SPONSOR/MONITOR'S REPORT NUMBER(S)
Grant 08-3049

12. DISTRIBUTION/AVAILABILITY STATEMENT

Approved for public release; distribution is unlimited.

13. SUPPLEMENTARY NOTES

14. ABSTRACT

This report results from a contract tasking National University of Ireland Maynooth as follows: Design and testing of dual-layer polarizers requires detailed research. Firstly, the polarizers usually operate in tilted orientation, which is relatively hard to simulate. Secondly, the finite conductivity of wires has to be taken into account, particularly, for tilted grids. Finally, other multi-grid structures (microstrip gratings) have to be analyzed as well (e.g., polarization-sensitive bolometers, whose analysis is needed for computing the ESA Planck telescope beams [8]).

A possibility of improving known devices or making new ones by using multi-grid structures (photonic crystals, left-handed meta-materials, etc) was noted long ago. Yet, subwavelength multi-layer grids received insufficient attention. Despite being used as circular polarizers, filters etc [4], these grids have not been considered as candidates for linear polarizers. In the meantime, inter-layer resonant effects in co-linear grids should significantly improve their performance.

15. SUBJECT TERMS

EOARD, Nanomaterials, terahertz technology, Nonlinear Optics

16. SECURITY CLASSIFICATION OF:			17. LIMITATION OF ABSTRACT	18. NUMBER OF PAGES	19a. NAME OF RESPONSIBLE PERSON
a. REPORT	b. ABSTRACT	c. THIS PAGE			A. GAVRIELIDES
UNCLAS	UNCLAS	UNCLAS	UL	31	19b. TELEPHONE NUMBER *(Include area code)* +44 (0)1895 616205

Standard Form 298 (Rev. 8/98)
Prescribed by ANSI Std. Z39-18

AQ F11-05-0627

European Office of Aerospace Research and Development

Grant Award

FA8655-08-1-3049

Final Report

Design, Manufacturing and Testing of Dual-Layer Frequency-Selective Subwavelength-Grid Polarizers of Enhanced Performance in THz Band

V. B. Yurchenko

NUI Maynooth, Ireland

9 September, 2009

1. Table of Contents

2. List of Figures

3. Summary

Design, manufacturing, and testing of dual-layer frequency-selective grid polarizers have been proposed for enhancing the polarizing efficiency of devices in the THz band as compared to conventional grids.

Dedicated software has been developed and numerical simulations carried out for the analysis of electromagnetic performance of a few kinds of dual-layer grid polarizers in the frequency range of up to 1 THz. Both free-space wire-grid and microstrip-grid structures on thin-film substrates in dual-layer assemblies have been simulated.

Dual-layer grid polarizers possess enhanced (squared) polarizing efficiency within extended frequency bands in transmission and at a sequence of discrete frequencies in reflection ("spike" frequencies) as compared to conventional single-layer grids. The operation frequencies can be tuned by either varying the inter-layer spacing in the assembly or tilting the polarizer plane with respect to the propagation direction of the incident wave.

An optimal design has been proposed for manufacturing and electromagnetic testing of polarizers with account of possible imperfections and manufacturing tolerances. A few sets of polarizer-analyzer pairs of dual-layer grid polarizers of the aperture diameter D=90mm and D=170mm have been fabricated for electromagnetic testing in the lower frequency band of 75-110 GHz and, at the later stage, in the high frequency band of 100-300 GHz.

Electromagnetic testing of dual-layer grid polarizers has been carried out in the frequency band of 75-110 GHz by using a VNA test facility at NUI Maynooth. Experimental data are shown to be in a good agreement with theoretical predictions. A steel-wire dual-grid polarizer of a robust design (of the wire thickness w=0.08mm and the grid period p=0.27mm) is shown to have the polarization extinction ratio of –65 dB to –55 dB in the frequency band of f = 75 - 110 GHz in transmission and about –60 dB at the "spike" frequency f = 95 GHz in reflection (at the beam incidence angle of 20 degrees, where both the "spike" frequency and the relevant incidence angle are defined by the grid interlayer spacing).

Thus, dual-layer grid polarizers of this kind, while having a very robust design, show an excellent performance that coincides with theoretical predictions and, when using slightly finer grids, are capable to operate efficiently in the relevant bands up to the terahertz frequencies.

4. Introduction

This work is concerned with development of enhanced dual-layer grid polarizers of record-breaking performance in THz and sub-THz bands as compared to conventional grids. Enhanced THz polarizers are needed in astrophysics (detection of polarization of Cosmic Microwave Background at the level about −80dB), polarization interferometry (space-borne defense-related systems), polarimetric remote sensing and security checks (target detection and recognition), spectroscopy (atmospheric research, chemical and pharmaceutical industry) and other areas.

Conventional grid polarizers dominated the area for many decades [1]. For today, however, this design has nearly exhausted its potential. Now, more advanced structures are needed, e.g., those based on chemically etched vertical or horizontal microstrip grids produced by special techniques (photolithography etc [2]), designed for exceptional performance in specific frequency bands, manufactured with extremely fine grids for THz and infrared systems, and optimized for particular applications.

Despite the availability of advanced technologies, manufacturing high-quality THz band polarizers is a complicated problem. Ideally, the finer grid, the better is the polarizer. In practice, conventional polarizers are limited in performance (extinction ratio can rarely exceed 30 dB) by finite conductivity and irregularities of grids [3], especially, in the THz band (finite conductivity imposes an absolute upper limit on grid efficiency). To overcome limitations, one needs to modify either entire system (use a dual-beam instead of rooftop interferometer [4]) or polarimetric unit (use a polarization-sensitive bolometer instead of a set of a separate polarizer and bolometer [5]).

A possible way of relaxing the limitations is the use of multi-layer grid structures (photonic devices) of subwavelength period of each grid, though of resonant inter-layer spacing. The latter should improve the polarizer performance and increase the efficiency in THz band when using relatively coarse grids of thick wires, which are less expensive and much easier to produce and operate.

Though multi-grid structures have been investigated for many microwave applications [6 - 9], there is only one report published recently that suggests a possibility of multiplication of extinction ratio of two polarizers in tandem [9]. In that instance, however, the authors based their conclusions on Mueller matrices of abstract polarizers that do not account for the correct self-consistent solution of the electromagnetic problem and, as a result, missed a range of frequency-selective properties (the fact that the extinction ratio increases at certain

frequencies while decreases at others, the dependence of the effect on transmission or reflection mode of operation, etc).

Computer simulation performed by our team earlier for certain dual-layer grids [10] predict a resonant growth of polarization extinction ratio (up to 80dB instead of the initial 40dB for some realistic design, in line with proposition [9]) which is expected in certain frequency bands or at particular frequencies, depending on either transmission or reflection mode of operation (a notion of strong frequency effects has been missed in [9]).

The aim of this work is to develop a practical design and undertake experimental manufacturing of a few sets of polarizer-analyzer pairs of dual-layer subwavelength-grid polarizers with subsequent experimental testing of their polarizing efficiency. The sets would include both the fine-grid devices for high-frequency (sub-THz) electromagnetic performance and relatively coarse model structures for detailed measurements of their polarization characteristics at relatively low frequencies in the band of f = 50 – 80 GHz and, at a later stage, in the band of f = 100 – 300 GHz.

5. Methods, Assumptions, and Procedures

Design and testing of dual-layer grid polarizers requires special research. Firstly, the polarizers usually operate in tilted orientation. Secondly, the finite conductivity of wires has to be taken into account. Finally, both the free-standing wire grids and microstrip gratings on thin-film dielectric substrates have to be analyzed as well (e.g., polarization-sensitive bolometers, whose analysis is needed for computing the ESA Planck telescope beams [11]).

A possibility of improving known devices or making new ones by using multi-grid structures (photonic crystals, left-handed meta-materials, etc) was noted long ago. Yet, subwavelength multi-layer grids received insufficient attention. Despite being used as circular polarizers, filters etc [6-7], these grids have not been considered as candidates for linear polarizers. In the meantime, inter-layer resonant effects in co-linear grids should significantly improve their performance.

In distinction from usual photonic structures and polarizers, we consider dual-layer grids with the following specific features: (a) grids have a subwavelength period, (b) wires are rather thick, and (c) wire conductivity is not so large.

The *advantages* of dual-layer grids are expected to be: (a) a significant increase of efficiency, even for the coarse grids of thick wires, (b) an increase of the upper limit of efficiency achievable with fine grids, (c) frequency-selective performance in either broad or narrow bands, (d) tuning the operation bands by varying the inter-layer spacing.

Meanwhile, potential *disadvantages* could be as follows: (a) more complicated manufacturing of these devices and (b) narrow bands of enhanced performance in certain operation modes (though, this could be an advantage for some applications).

Assuming the normal plane-wave incidence, perfect conductivity of wires, subwavelength period of grids and other approximations [10], we can estimate the expected performance of dual-grid polarizers in comparison to single grids of similar kind. The estimates show a significant growth of extinction ratio (e.g., from 30 to 60 dB at the wire diameter d=0.1 mm) that occurs at certain frequencies or frequency bands, depending on the operation mode.

Now questions arise to what extent these effects will be observed in real dual-layer grids of finite conductivity, how well can the grids operate as 3dB polarization splitters, how can they behave at oblique incidence of electromagnetic wave, what will be the effects of imperfections, etc. The research answers these questions and allows us to develop efficient dual-layer grid polarizers for THz applications.

5.1. Simulation Methods

5.1.1. Approximate Asymptotic Models

Developing THz and sub-THz polarizers is a challenging issue because of constrained manufacturing and operation requirements. Numerical simulations allow one to optimize the design of dual-layer grid structures with account of realistic parameters of devices and their operation conditions.

As a basic option, our computations utilize the analytical form of stand-alone wire grid effective layer boundary conditions obtained by Wainshtein [12]. The boundary conditions [12] relate the averaged (smoothed) values of the electric and magnetic fields on the opposite sides of a dense subwavelength wire grid for two orthogonal polarizations of the incident electromagnetic wave as follows:

$$\begin{aligned} E_y^{+\delta} + E_y^{-\delta} &= 2R_Y(H_x^{+\delta} - H_x^{-\delta}) & E_x^{+\delta} + E_x^{-\delta} &= -2R_X(H_y^{+\delta} - H_y^{-\delta}) \\ H_x^{+\delta} + H_x^{-\delta} &= 2S_Y(E_y^{+\delta} - E_y^{-\delta}) & H_y^{+\delta} + H_y^{-\delta} &= -2S_X(E_x^{+\delta} - E_x^{-\delta}) \end{aligned} \qquad (5.1)$$

where $E_{x,y}^{+\delta}$, $E_{x,y}^{-\delta}$, $H_{x,y}^{+\delta}$, $H_{x,y}^{-\delta}$ are the relevant components of the electric and magnetic fields at the opposite sides of the grid (taken at the distance δ greater than the grid period p, though small as compared to the wavelength λ and the inter-grid spacing d) and $R_{X,Y}$, $S_{X,Y}$ are the effective boundary coefficients for the relevant polarizations of the incident waves with respect to the grid wires as shown in Fig. 5.1.

Figure 5.1. A dual-layer grid polarizer in the case of E polarized wave incidence (E field of the wave incident from the left is parallel to the grid wires, while being parallel to the X axis)

A solution proposed by Wainshtein [12] provides analytic formulae for a complete set of four coefficients in the relationships of the kind of Eqs. (5.1) that can be represented in terms of coefficients $R_{X,Y}$, $S_{X,Y}$ defined above.

The formulae specify coefficients $R_{X,Y}$, $S_{X,Y}$ as functions of the grid period p, the wire thickness w and the conductivity of the wire material σ under the condition of good conductivity of wires and subwavelength period of grids ($p << \lambda$).

In addition, the formulae provide options for different shape of metallic wires by considering either grids of circular cylindrical wires or lateral microstrip gratings. In the latter case, we can compare simulations of dual-layer gratings with a more rigorous approach based on regularization method (see below), and the comparison shows a remarkably good similarity of two solutions.

The formulation of this kind is well justified for subwavelength grids, since the waves around the grid restore their homogeneous structure at the distance which is greater than the grid period, though small as compared to both the wavelength and the inter-grid spacing.

By using these boundary conditions, one can easily evaluate, as a self-consistent electromagnetic solution, both the transmission and refection coefficients of any composite structure made of a few layers of grids of any orientation and a few layers of dielectric materials, for any polarization and inclination of the incident waves. When simulating dual-layer grid structures, this allowed us to account for the generic tilt of grids with respect to the incident waves, finite conductivity of wires, finite width of radiation beams etc.

The approach has been implemented in the computer software in such a form that one can easily combine any kinds of layers in any order and compute the entire structure performance (e.g., the efficiency of a stack of layers as a Bragg mirror polarizer) by direct multiplication of relevant matrices, with a possibility of automatic optimization of the whole structure with respect to the given parameters.

Simplified models could become erroneous for dual grids of small inter-layer spacing or at the resonant conditions. Therefore, at the later stage, for the detailed comparison of numerical simulations with experimental data, we shall develop a special code based on exact solutions for tilted wires of finite conductivity, when there is no independent TE and TM propagation modes. An important part of this simulation will be the use of super-convergent lattice sum techniques proposed in Ref. [8].

For thin wires, one can neglect higher-order angular modes. Notice, however, that earlier, when simulating a grid cage [13], we found that both n=0 and n=1 modes (but no more) are needed, where n=1 terms become significant near the resonances. A similar effect is expected in the dual grids as well.

5.1.2. Simulations Based on Regularization Methods

For simulations of microstrip gratings, we have developed a software code based on regularization methods [10, 14]. The key element of this software is the use of analytical inversion of singular part of relevant scattering problem that makes a numerical solution of the entire problem well-defined, rapidly convergent, and easily computed [14].

Mathematically, it means a transformation of the original ill-posed problem of solving Fredholm equations of the first kind into the well-posed associated problem represented by the Fredholm equations of the second kind [15, 16]. The application of this procedure is a necessity when solving scattering problems for the conductive bodies with sharp edges, including the metallic strip gratings [14].

When applying the technique to subwavelength gratings, we can obtain sufficiently accurate values of the effective coefficients $R_{X,Y}$ and $S_{X,Y}$ that describe the electromagnetic effects of gratings in terms of the effective boundary conditions represented by Eqs. (5.1). Then, the dual-layer microstrip grating problem is being solved along the same lines as described above in the case of dual-layer wire grids.

It is this kind of simulations that have been made for dual-layer microstrip gratings at the given stage of research. The approach also allows us to account for the effect of dielectric substrates that are necessary for polarizers made of microstrip gratings.

Alternatively, regularization procedure can be developed for the entire problem of the dual-layer (and, indeed, multi-layer) stacks of microstrip gratings on dielectric substrates. This could be of interest for the detailed comparison of simulations with experimental data at the later stages of this research.

5.2. Manufacturing Procedures

5.2.1. Wire-Grid Dual-Layer Assemblies

In manufacturing, the simplest option is to make wire-grid polarizers. It is widely available and inexpensive method. Though photolithographic techniques are more advanced, they are more expensive and not as readily available.

It is expected that, when using a steel-core silver-coated wire of sufficiently small diameter w (w < 0.1 mm), a range of dual-layer wire-grid polarizers could be produced which should be suitable for experimental testing at the frequencies of about 100 GHz (with the radiation wavelength of 3 mm). With the use of tungsten wires of smaller diameter (down to 0.01 mm) the range is supposed to be extended to the higher frequency bands.

An important requirement to the polarizers of enhanced polarizing efficiency is to have a sufficiently large aperture area in order to accommodate the entire radiation beam. The basic estimate is that, assuming the polarization extinction ratio at the level of, e.g., 60 dB, the entire beam down to the level of -60 dB has to fit into the aperture with account of possible tilt of the polarizer with respect to the beam axis at the actual operation position.

In addition, high accuracy of manufacturing is required to reduce imperfections that may degrade the polarizer performance. These conditions impose constrained requirements on manufacturing tolerances that have to be met in the fabrication process (specific data based on our simulations are presented below in Sections 6.2 and 6.3).

5.2.2. Microstrip Gratings on Thin-Film Substrates

As an alternative, other design and manufacturing options such as chemical etching of microstrip gratings on thin-film low-loss dielectric substrates is considered. A possibility for making microstrip gratings of such a kind is available at the Tyndall National Institute (Cork, Ireland), and the relevant technology is being explored.

5.3. Electromagnetic Characterization Options

5.3.1. Open-Resonator Techniques

Electromagnetic testing of dual-layer polarizers of enhanced performance at the frequencies exceeding 100 GHz is a particularly challenging issue when the polarization extinction ratio can reach or exceed 40 – 50 dB.

The best approach to solving this problem is supposed to be the use of the open-resonator techniques that have successfully been developed in recent time for the purpose of measuring extremely low absorption losses in ultra-low-loss dielectric materials [17].

When using an open resonator with the quality factor $Q \sim 10^6$, absorption at the level as low as -60 dB can be detected [17] that shows a possibility of detecting the polarization extinction ratio at the same level as well. As an alternative, an open resonator with $Q \sim 10^4$ is available for similar measurements (f = 50–150 GHz) at the IRE NASU (Kharkov, Ukraine).

The open-resonator method has to be extended for the case of tilted orientation of a polarizer and for the measurements to be carried out in both transmission and reflection mode of operation. This requires generalization of both the formulations and software needed for the data processing and the parameter extraction as compared to those being used in the dielectric absorption measurements.

5.3.2. Free-Space Beam Propagation Method

A straightforward way of measuring high-frequency electromagnetic performance of a polarizer-analyzer pair is the use of free-space beam propagation method (Fig. 5.2).

In this method, the beam is propagated from the source S through a set of two polarizers P1 and P2 towards the detector T in transmission mode and partially reflected from the polarizer P2 towards the detector R in reflection mode. The dual-layer polarizer P1 (identical to the polarizer P2) is preparing the beam of sufficient polarization purity, which is used as the beam incident on the polarizer P2 at a certain angle θ.

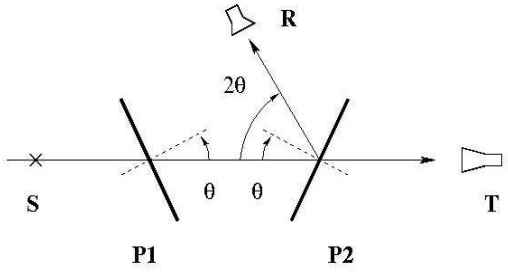

Figure 5.2. Schematics of a free-space beam propagation method for high-frequency electromagnetic testing of a polarizer-analyzer pair (P1 and P2) in reflection (R) and transmission (T) configurations (S is the source of the radiation beam propagating towards the detector T)

When the polarizer P2 is absent, detector T receives a calibration signal, which is used for normalization purposes. When the polarizer P2 is present and the polarization directions of both P1 and P2 are co-aligned so that propagation signal received by the detector T is at maximum, the reflection signal received by the detector R is at minimum. On the contrary, when the polarizer P2 is twisted by 90 degrees about its axis (dotted line) so that both the polarizers P1 and P2 are cross-aligned, the propagation signal at the detector T is at the minimum and the reflection signal at the detector R is at the maximum.

Now, by taking the ratios of different normalized signals received by detectors T and R in these two orthogonal configurations, one can directly evaluate various polarization extinction ratios and other quantities as shown below in Figs. 6.1-6.5 and compare them with theoretical prediction obtained by simulations.

An essential requirement in this method is the need to have a well-collimated beam and relevant angular sensitivity patterns of detectors R and T, along with sufficient aperture diameters of polarizers P1 and P2, so that no edge diffraction effects could contaminate the measurements at so low level of signals as expected in this experiment.

6. Results and Discussions

6.1. Simulations

6.1.1. Free-Space Wire-Grid Dual-Layer Structures

The model developed in our simulations takes into account both the geometrical parameters of grids (the wire diameter w, the grid period p, the inter-layer spacing d) and the electrical conductivity σ of wires (the model assumes $d \sim \lambda >> p$ where λ is the radiation wavelength) [18].

For the purpose of manufacturing and electromagnetic testing of wire-grid polarizers in the frequency band of f = 50 – 80 GHz available in the experiment (λ = 6.00 – 3.75 mm), we simulated dual-layer grid structures characterized by the following set of parameters: w = 0.08 mm, p = 0.32 mm, d = 1.3 mm, and $\sigma = 10^7$ Sm/m (Figs. 6.1– 6.5).

Keeping in mind essential systematic effects common for experimental and real operation conditions (a limited beam width of radiation in connection with angular dependence of polarizer performance), both the uniform plane wave (curves “n_1” and “n_2”) and the actual Gaussian beam excitation typical for the experiment (curves “ns_1” and “ns_2”) have been considered and taken into account.

Computer simulations reveal the following properties which are common for all kinds of dual-layer grid polarizers [18, 19]:

(a) a significant (quadratic) growth of polarization ratio in reflected waves (the ratio $R_{RE} = E_R / H_R$ of reflected amplitudes for the incident E- (co-) and H- (cross-) polarized waves when either E or H field is parallel to grid wires) that happens at certain "spike" frequencies f_n (Fig. 6.1, a),

(b) a similar quadratic growth of polarization ratio in transmitted waves (the ratio $R_{TR} = H_T / E_T$ of transmitted amplitudes for the incident H- (cross-) and E- (co-) polarized waves) that occurs in broad frequency bands centered around the "spike" frequencies f_n (Fig. 6.1, b),

(c) a similar kind of effects for polarization ratios defined by relating reflected and transmitted waves of the same incident polarization, $R_H = H_T / H_R$ and $R_E = E_R / E_T$, respectively (Fig. 6.2, a and b),

(d) a precise 3dB splitting of the incident non-polarized beam into reflected and transmitted polarized waves that occurs at the "spike" frequencies f_n regardless of the parameters of separate grids (Fig. 6.3, a),

(e) a significant resonant absorption that occurs at the resonant frequencies f_n^{RES} (Fig. 6.3, b), that, however, is not critical, since the structure is not going to be used at the resonant frequencies.

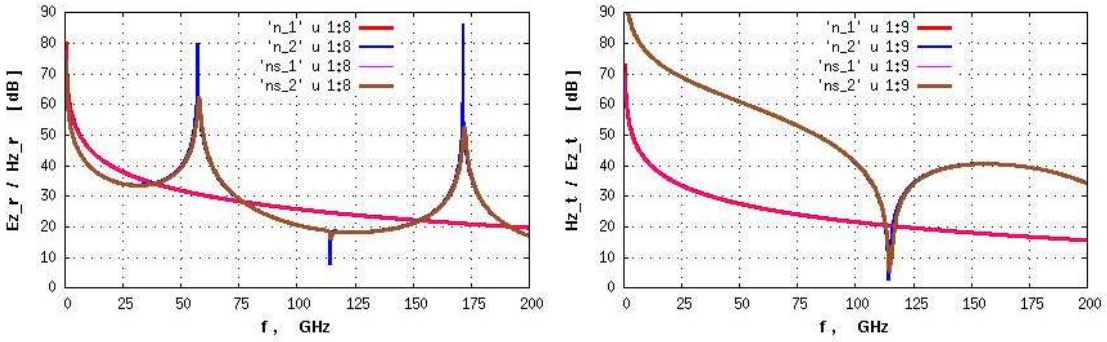

(a) (b)

Figure 6.1. Polarization ratio (a) $R_{RE} = E_R / H_R$ and (b) $R_{TR} = H_T / E_T$ defined by considering reflected and transmitted waves at relevant polarizations of the incident field in the case of single-layer (n1, ns1) and dual-layer grids (n2, ns2) under the plane wave (n1, n2) and the Gaussian beam (ns1, ns2) excitation

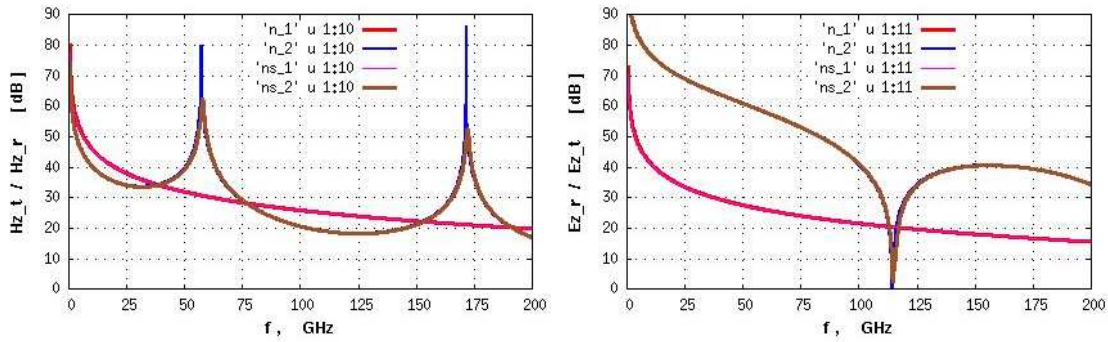

(a) (b)

Figure 6.2. Polarization ratio (a) $R_H = H_T / H_R$ and (b) $R_E = E_R / E_T$ defined by relating reflected and transmitted waves of the same incident polarization

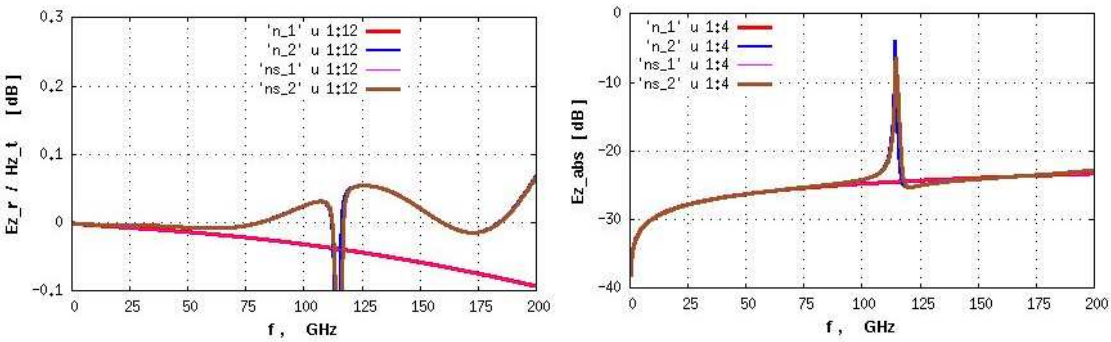

(a) (b)

Figure 6.3. (a) Polarizing beam power splitting and (b) power absorption by a dual-layer (n2, ns2) and a single-layer (n1, ns1) grid structure

Figures 6.4 and 6.5 explain the enhancement of dual-layer grid polarizers by showing the frequency dependence of reflected and transmitted power of co- and cross-polarized waves.

The reason for the enhancement of polarizing efficiency is the suppression of (small) reflected cross-polarized component (H wave, with E field orthogonal to grid wires) and transmitted co-component (E wave, with E field parallel to grid wires) that occurs due to destructive interference of relevant waves. This happens at the "quarter-wave-plate" condition on the inter-grid spacing $d = (2n-1)\,\lambda / 4$ where $n = 1, 2, 3, \ldots$. This is precisely the condition of "spike" frequencies f_n .

Meanwhile, conventional half-wavelength resonant frequencies ($d = n\,\lambda / 2$) correspond to the dips of polarizing efficiency due to increased transparency of dual-layer grids for co-polarized waves at the resonant conditions.

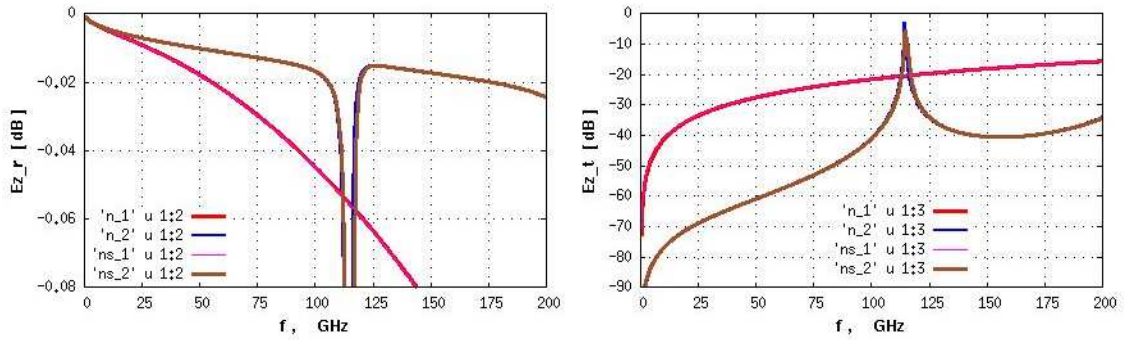

(a) (b)

Figure 6.4. (a) Reflected and (b) transmitted waves of E polarization in the case of single-layer and dual-layer grids

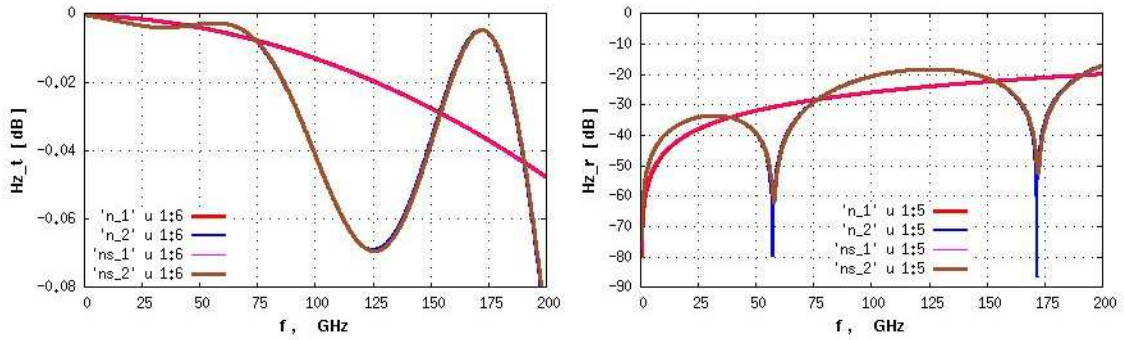

(a) (b)

Figure 6.5. (a) Transmitted and (b) reflected waves of H polarization in the case of single-layer and dual-layer grids

6.1.2. Thin-Film Microstrip-Grating Dual-Layer Structures

A more rigorous approach has been developed for simulating microstrip gratings on dielectric substrates by using regularization methods with account of absorption in gratings and substrates (Figs. 6.6 – 6.10) [19].

Thin-film microstrip-grating dual-layer polarizers are shown schematically in Fig. 6.6. Parameters of two kinds of polarizers that have been simulated and supposed to be manufactured are summarized in Table 6.1

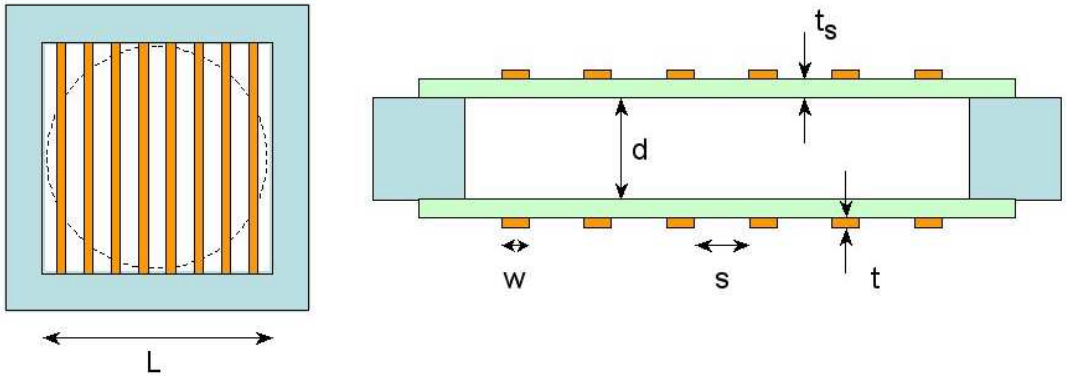

(a) (b)

Figure 6.6. Schematics of a dual-layer polarizer with microstrip gratings on thin-film low-loss dielectric substrates: (a) top view, (b) side view

Table 6.1. Parameters of thin-film microstrip-grating dual-layer polarizers

Grating #	**Strip Width** w, μm	**Slot Width** s, μm	**Period** p, μm	**Spacing** d, μm
1	6	14	20	500
2	80	120	200	700

Computer simulations were carried out for copper gratings of Table 6.1 assuming the use of dielectric substrates of 12 μm Mylar film with loss tangent of about 0.01 (copper cladding of 2 μm thickness is simulated as an infinitesimal thin screen in this model).

Thin-film substrates of low-loss dielectrics do not substantially affect the polarizer performance in transmission mode. In reflection, however, they produce non-polarized waves that may noticeably degrade the device (Fig. 6.7, a). Despite this negative effect (which is small for thin substrates), the enhanced polarizing performance in reflection at the ”spike”

frequencies f_n is, typically, higher for the dual-layer grids on film substrates as compared to similar single-layer grids suspended in free space.

Figures 6.8 and 6.9 illustrate the enhancement of dual-layer microstrip polarizers by showing the frequency dependencies of reflected and transmitted power of co- and cross-

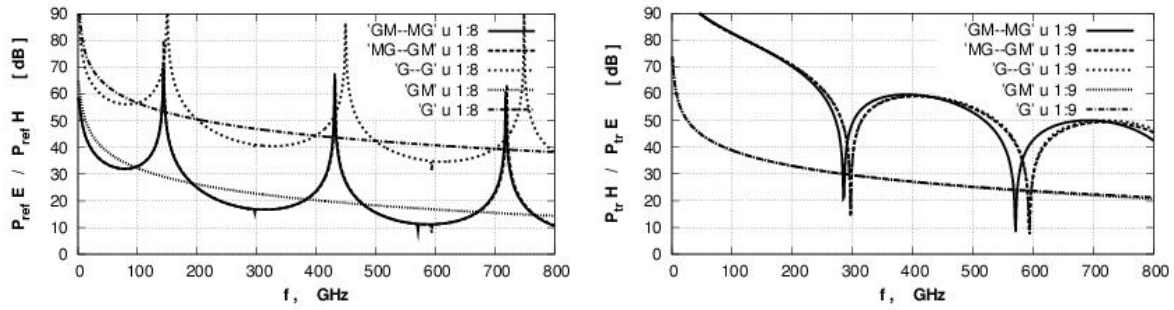

(a) (b)

Figure 6.7. Extinction ratio in reflected and transmitted waves for polarizers of gratings #1 on Mylar substrates when gratings are made on either the outer (GM-MG) or the inner (MG-GM) faces as compared to free-standing dual-layer (G-G) and single-layer (GM and G) grid polarizers

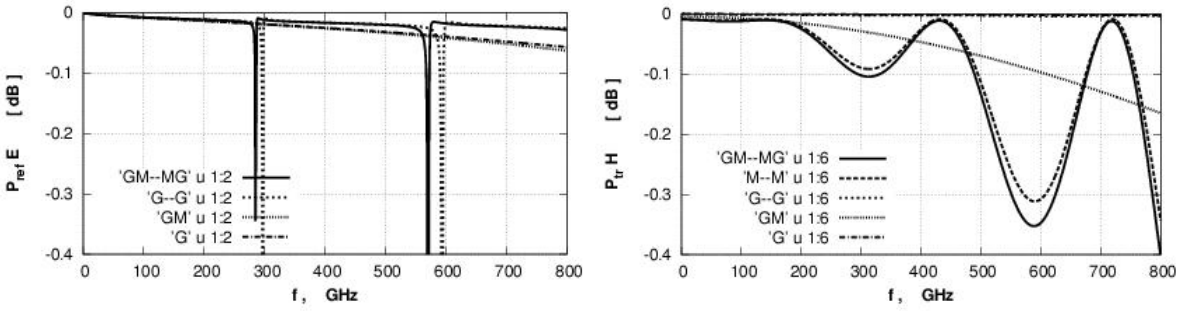

(a) (b)

Figure 6.8. Reflected power in (a) co- and (b) cross-polarization (E and H waves, respectively) that explains the spikes of enhanced polarization in Fig. 6.7, a

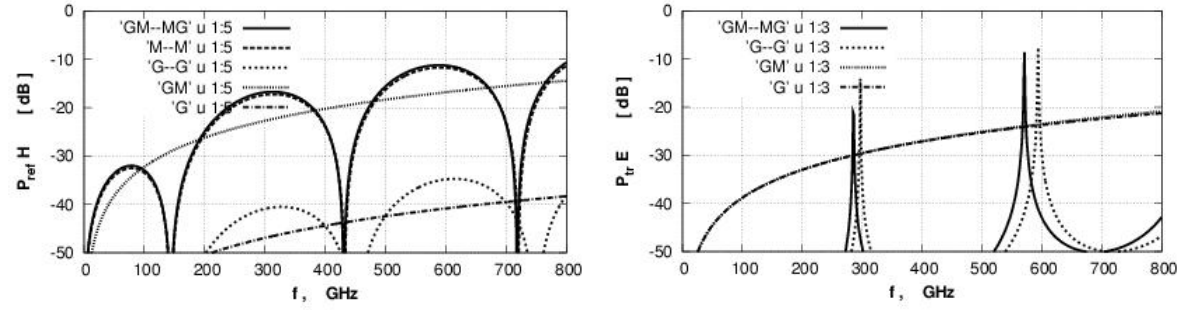

(a) (b)

Figure 6.9. Transmitted power in (a) cross- and (b) co-polarization (H and E waves, respectively) that explains broad bands of enhanced polarization in Fig.6.7, b

polarized waves. The curves are similar to those of the wire-grid structures, though they show some depolarizing effect arising due to reflection from thin-film substrates.

Thus, by using gratings of period p and strip width w so that cross-polarized reflectance is reduced versus co-polarized transparency in free-space while being comparable on substrates, one can increase the polarizing efficiency of dual-layer grids on substrates at "spike" frequencies in both reflection and transmission (if a beam splitters is needed) and within extended bands in transmission. This is the condition satisfied by gratings #1.

An interesting feature of a dual-grid polarizer is an exact half-power splitting of a non-polarized beam into reflected and transmitted polarized waves that occurs at the "spike" frequencies regardless of the grid parameters. For a coarse-grid dual-layer polarizer (#2), exact half-power splitting occurs at the "spike" frequencies only (Fig. 6.10, a) whereas for fine grid structures (#1) it remains accurate within the entire bands of enhanced polarized transmission.

Another feature typical for all resonant structures is a rapid increase of absorption at the resonant frequencies (Fig. 6.10, b), though it is of minimal importance for these devices since it happens at the dips of their polarizing performance.

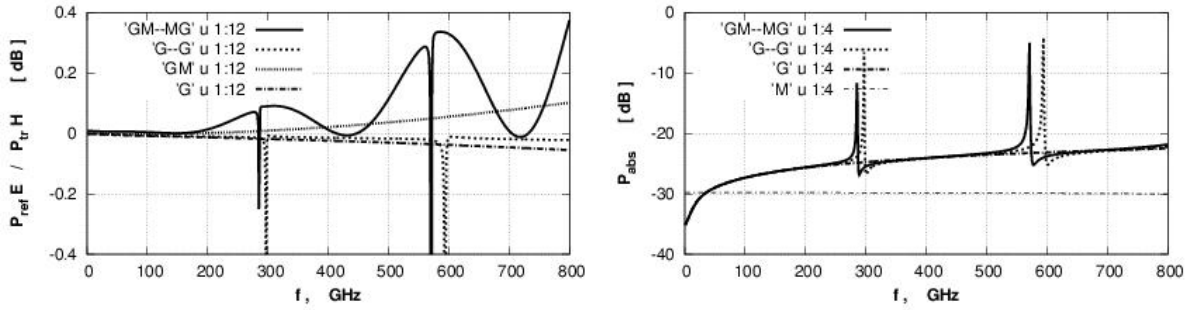

(a) (b)

Figure 6.10. (a) Polarizer as a 3dB power splitter and (b) power absorbed by a dual-layer polarizer as a function of frequency (coarse gratings #2)

All the results above are shown for the case of normal incidence of the electro-magnetic wave on the polarizer plane. When the wave is incident at an angle θ with respect to the normal to the polarizer plane, all the characteristic spike and dip frequencies $f_n(\theta)$ are shifted from their original positions according to the equation

$$f_n(\theta) = f_n(0) / \cos\theta \qquad (6.1)$$

where $f_n(0)$ is the relevant frequency at the normal wave incidence (the equation is valid in a limited range of angles where the asymptotic model based on Eqs. (5.1) is justified).

6.2. Manufacturing

6.2.1. Manufacturing Requirements and Tolerances

Manufacturing requirements on the design of polarizer, the aperture size, the accuracy and mechanical tolerances etc, depend on the type of structure (a wire grid or microstrip grating) and on the frequency band to be used. Basic requirements and considerations behind them should be evaluated specifically for each kind of structure and experimental conditions.

As an example, consider a wire-grid dual-layer polarizer presented in Section 6.2.2, which is manufactured for electromagnetic testing in the frequency band of f=50–80 GHz with an open resonator described in Section 6.3.1. As a first step, in order to formulate basic requirements, we should evaluate unavoidable effects of the finite Gaussian beam width and angular divergence. They define the minimum aperture diameter acceptable for the polarizer (D = 90 mm in this example, see Section 6.3.1) and the maximum polarization extinction ratio achievable at the spike frequencies (described below).

The angular divergence of Gaussian beam (estimated to be in the range of 20 – 16 degrees in the frequency band of f = 50–80 GHz in this example) imposes an upper limit on polarization extinction ratio at the "spike" frequencies in reflection (this is due to the angular dependence of spike frequencies described by Eqn. (6.1)) as compared to the plane wave incidence, though no reduction of polarization is observed in transmission (other imperfections, e.g., non-uniform inter-layer spacing, produce similar effects).

In this case, for the given dual-layer polarizer and beam parameters, we obtain the same polarization ratio at the "spike" frequency f_1 = 57.7 GHz at the level of 60 dB in both reflection and transmission (brown curves in Figs. 6.1 – 6.5) as compared to 30 dB for a similar grid of a single-layer device (magenta curves).

These values were obtained by properly adjusting the wire grid parameters (the wire thickness w, the grid period p, and the inter-layer spacing b of the dual-layer grid structure) and choosing them, eventually, as they were specified in our simulations in Section 6.1.1 above (w = 0.08 mm, p = 0.32 mm, d = 1.3 mm).

In a similar way, when considering a polarizer made of microstrip gratings on thin-film substrates, one should account for depolarizing effect of substrates that reduces the polarization extinction ratio in reflection in addition to the Gaussian beam divergence effect. Then, the microstrip grid parameters are adjusted as to achieve a comparable polarization extinction ratio at the spike frequencies in both reflection and transmission when the polarizer has to operate as a beam splitter (fine gratings # 1 in Table 6.1, Fig. 6.7).

6.2.2. Wire-Grid Dual-Layer Assemblies

A few sets of polarizer-analyzer pairs of dual-layer wire-grid polarizers of different aperture diameter (D=90mm and D=170mm) have been fabricated for electromagnetic testing in the lower frequency band of 75-110 GHz and, at the later stage, in the higher frequency bands of 100-300 GHz (Fig. 6.11-6.13).

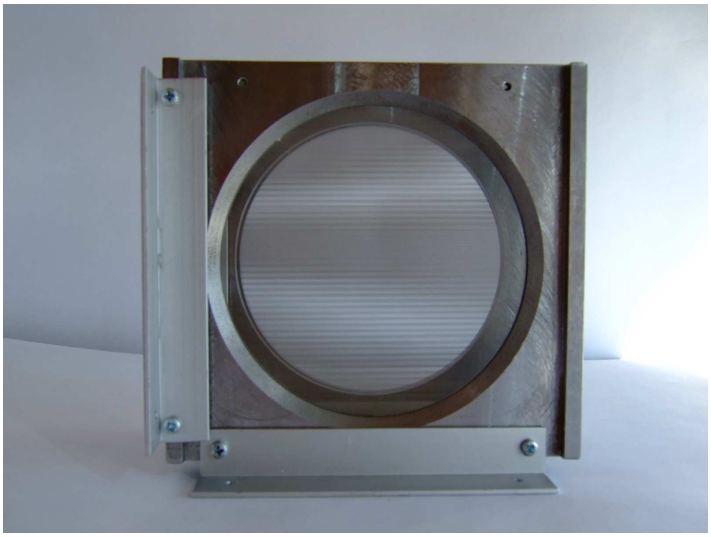

Figure 6.11. Two dual-layer grid polarizers in tandem (w=0.08mm, p=0.27mm, d=0.8mm, D=90mm) with a Moire pattern visible due to four grids overlapping in the aperture area (a second polarizer is slightly tilted with respect to the line-of-sight)

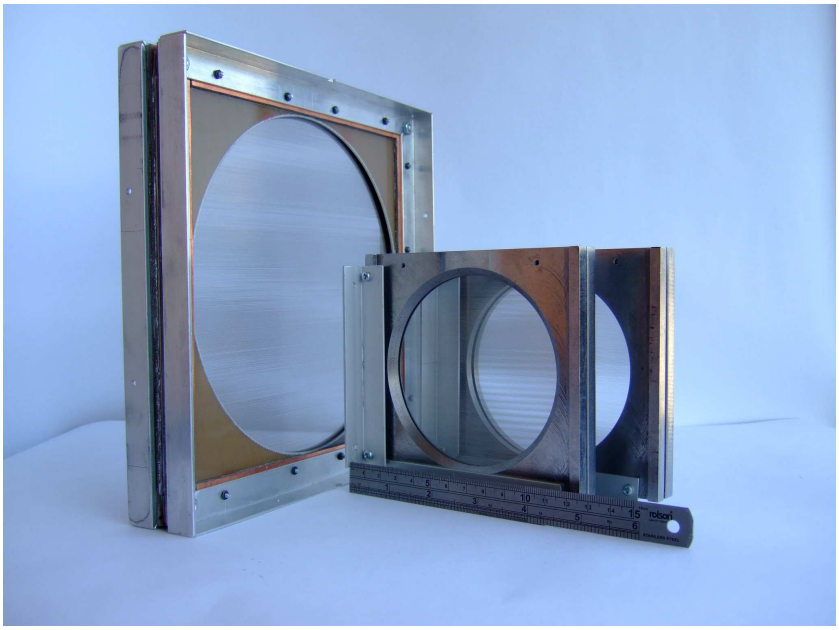

Figure 6.12. Moire patterns in the apertures of dual-layer polarizers show sufficient quality of grids. A more complicated second-order pattern in the overlapping apertures of small polarizers (D=90mm in both Figs. 6.11 and 6.12) is due to the interplay between four identical grids

Each polarizer has been made as an assembly of two parallel wire grids stretched over the frame of appropriate aperture and thickness. The grid parameters are chosen to be as follows: w = 0.08 mm, p = 0.27 mm, d = 0.80 mm and the aperture diameter D=90mm for the polarizers of one kind (small-aperture polarizers), and w = 0.09 mm, p = 0.33 mm, d = 1.00 mm and the aperture diameter D=170mm for the polarizers of another kind (large-aperture polarizers).

The grids in each assembly were made to be sufficiently planar and parallel, with non-planarity and non-parallelism of grid planes less than plus-minus 0.02 mm over the aperture area. This requirement on the uncertainty of inter-layer spacing allows us to keep polarization ratio at the "spike" frequencies in reflection at the same level of 60 dB as in transmission. Then, spectral curves of polarization extinction ratio at the plane wave incidence with account of this imperfection look the same as the curves computed for the perfect structure at the Gaussian beam incidence (brown curves in Figs. 6.1 – 6.5).

Similarly, misalignment of wires of two grids is made to be better than 3 arcminutes that corresponds to misfit of wires of different grids by about w = 0.08 mm (about one wire diameter) at one end of the grid pair as compared to the other end (assuming the grid aperture size D = 90 mm).

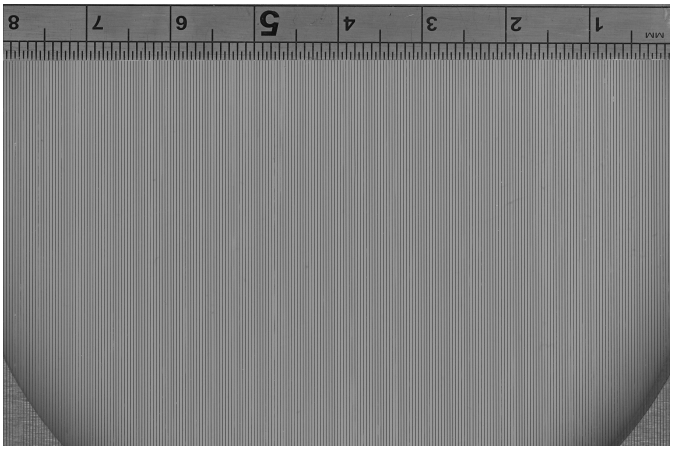

Figure 6.13. An example of a grid available at the early stage of the project

Quality of grids can be seen by observing the Moire patterns that appear due to the interplay between four identical grids when overlapping the apertures of two polarizers in tandem as shown in Figs. 6.11 and 6.12. An example of a grid available at the early stage of the project is shown in Fig. 6.13.

Wire-grid polarizers of this kind have a very robust design. They are supposed to be well suited for low-loss high-power applications, yet providing, according to our results, a sufficiently high polarizing performance (at the level of –60dB of polarization extinction ratio) in the frequency band around f=100 GHz where electromagnetic testing has been made.

6.3. Electromagnetic Testing

6.3.1. Electromagnetic Testing Requirements

A pair of dual-layer polarizers that constitutes one polarizer-analyzer set is needed for polarization experiments. Dual-layer polarizers made of the wire grids described above have been tested in the frequency band of f=75–110 GHz by free-space beam propagation method (see Section 5.3.2 above) using vector-network-analyzer (VNA) high-frequency test facility operating at the NUI Maynooth.

Requirements for high-frequency testing of enhanced polarizers are demanding. In addition to precise positioning of polarizers in cross-orientation with accuracy better than 3 arcminutes for maintaining spurious signals below –60dB, detection of signals of ultra-low level is needed. As a possible solution, one may use a resonator technique being developed for electromagnetic testing of ultra-low-loss materials [17] as mentioned in Section 5.3.

If using an open resonator designed for the frequency band of f=50–80 GHz, which consists of two concave mirrors of diameter D_M =100 mm and the curvature radius R_M =110 mm placed at the distance L_M =160 mm one from another, one obtains a Gaussian beam of half-width w_0 =10–7.5 mm at the beam waist and w_M =20–15 mm at the resonator mirrors.

The beam of this kind is characterized by the angular divergence of 20–16 degrees and maintains a spurious signal at the rim of the grid aperture of typical size D = 90 mm at the level below –60 dB while having the grid in the middle of the resonator tilted at 45 degrees with respect to the resonator axis (at the normal grid orientation, the grid aperture size has to be D > 52 mm at the beam waist and D > 104 mm at the resonator mirrors).

When expressing electromagnetic properties of a subwavelength grid in terms of homogenized parameters, one can compute the effective permittivity of grid in both co- and cross-polarized orientations (in co-polarization, the effective permittivity is negative and resembles the permittivity of plasma below the plasma frequency). Then, by measuring the effective permittivity of a dual-layer grid, one can verify the electromagnetic parameters of the entire structure against numerical simulations.

An alternative representation of the same data is the plot of complex scattering matrix coefficients S_{11}, S_{12} that shows specific features of resonant behavior of dual-layer grid polarizers, thus providing both the qualitative and quantitative characterization of the devices.

Requirements for the free-space beam propagation method (Section 5.3.2) are no less demanding. As mentioned earlier, in this method, a very significant requirement is the need to have a well-collimated beam, narrow angular patterns of detectors R and T, and sufficiently large aperture diameters of polarizers, so that no edge effects could contaminate the measurements at so low level of signals as expected in this experiment.

In order to satisfy all these requirements, a special set of quasi-optical focusing elements (ellipsoidal reflector mirrors with extra dual-layer polarizers at both the source and detector sites) had to be applied that appeared to be a crucial development, especially, when measuring reflected signals from the polarizer by the detector R in the case of oblique beam incidence (see Fig. 5.2 above).

6.3.2. Results of Dual-LayerGrid Polarizer Measurements with Beam Propagation Method

The results of high-frequency electromagnetic testing of dual-layer grid polarizers in both transmission and reflection configurations are summarized in Fig. 6.14. The results are presented for the polarizers of small diameter (D=90mm, w=0.08mm, p=0.27mm) at oblique wave incidence ($\theta \sim 20$ degrees, d=0.8mm).

Curves 1 to 4 in Fig. 6.14 show the power in dB of the signal received by the relevant detector (R or T) versus frequency in GHz in the following configurations, respectively:

1 - signal going through in co-polar grid position of the polarizer P2 (horizontal grid parallel to H-field, large signal going through),

2 - signal reflected in cross-polar grid position of the polarizer P2 (vertical grid parallel to E-field, large signal reflected),

3 - signal reflected in co-polar grid position of the polarizer P2 (horizontal grid parallel to H-field, small signal reflected),

4 - signal going through in cross-polar grid position of the polarizer P2 (vertical grid parallel to E-field, small signal going through).

All the curves represent the signals normalized with respect to the calibration signal received by detector T when only one polarizer P1 is present as explained in Section 5.3.2.

For the comparison, smooth curves (light-blue and brown ones) show the simulation results obtained for the polarizers of this kind at the oblique beam incidence.

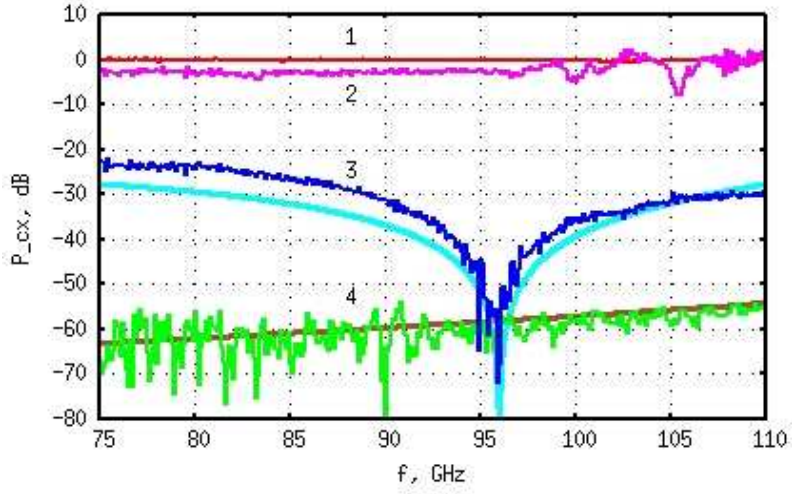

Figure 6.14. Results of high-frequency measurements for the polarizers of small diameter (D=90mm) in comparison to simulations (the meaning of curves is explained in the text)

The measurements show that, for the dual-layer grid polarizer of such a robust design, polarization extinction ratio is achieved at the level of –65 dB to –55 dB in the frequency band of f = 75-110 GHz in transmission and about –60 dB at the "spike" frequency f = 95 GHz in reflection (at the beam incidence angle of 20 degrees, where both the "spike" frequency and the relevant incidence angle are defined by the grid interlayer spacing).

Polarization extinction ratios that can be achieved, according to simulations, by these polarizers and the polarizers of a finer grid (w=0.02mm, p=0.08mm) in a broader frequency range are shown, for the comparison, in Figs. 6.15 and 6.16.

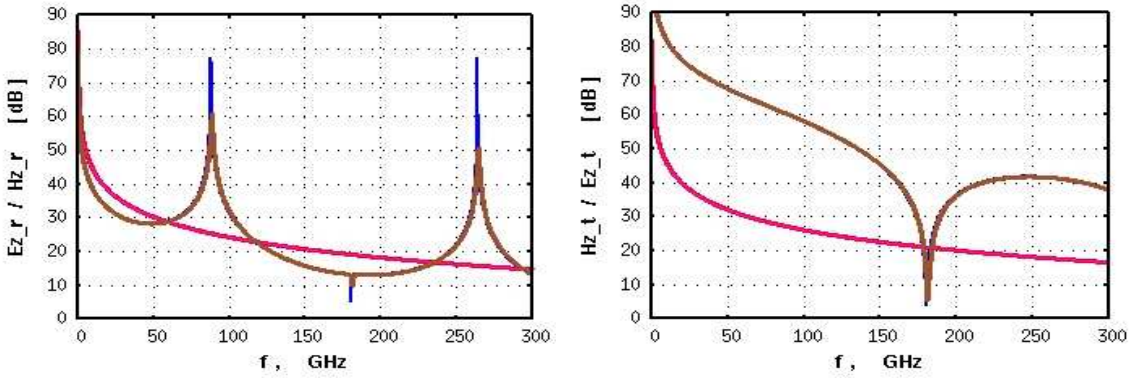

Figure 6.15. Polarization extinction ratios that can be achieved, according to simulations, by the polarizers of Fig. 6.14 (w=0.08mm, p=0.27mm) in the frequency range up to f = 300 GHz

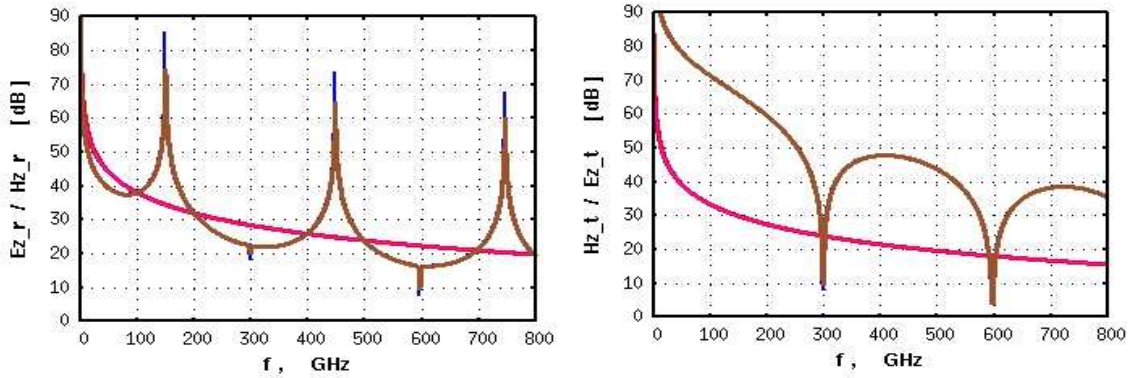

Figure 6.16. Polarization extinction ratios that can be achieved, according to simulations, by the polarizers of a fine grid (w=0.02mm, p=0.08mm) in the frequency range up to f = 800 GHz

When being used as the polarizing beam splitters, they would be able to show the performance as illustrated by Fig. 6.17, a and b, respectively.

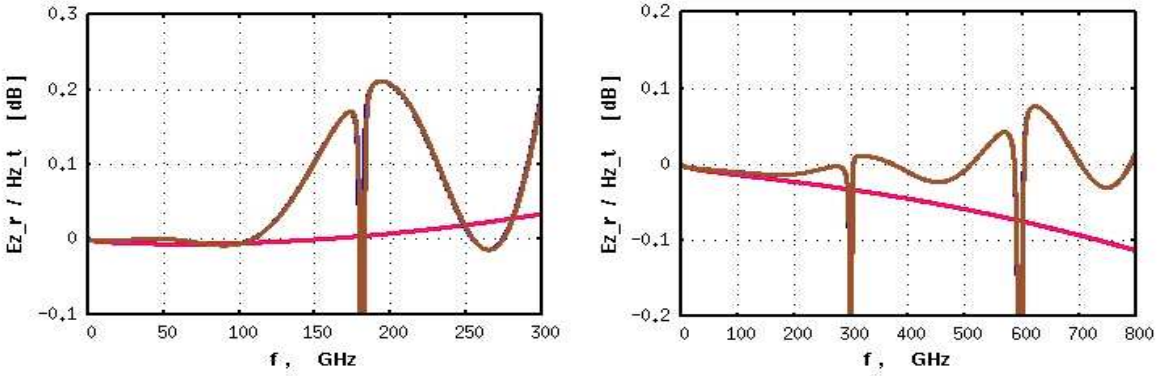

Figure 6.17. Polarizers of (a) Fig. 6.15 and (b) Fig. 6.16 when operating as the beam splitters

Thus, the results of high-frequency measurements of dual-layer wire-grid polarizers confirm theoretical predictions made with our simulation model and show a significant enhancement in the performance of this kind of polarizers in both transmission and reflection configurations over conventional single-layer grids of similar design.

7. Conclusions

Dual-layer grid polarizers have been proposed for achieving an enhanced polarizing efficiency in THz and sub-THz bands as compared to conventional single-grid structures.

Dedicated software has been developed and numerical simulations carried out for the analysis of electromagnetic performance of dual-layer grid polarizers in a broad frequency range extending up to 1 THz. Both free-space wire-grid and microstrip-grid structures on thin-film substrates in dual-layer assemblies have been simulated.

Dual-layer grid polarizers have the following advantages over conventional grids:

(a) a large increase of polarizing efficiency (polarization extinction ratio squared as compared to conventional devices) even in the case of coarse grids of thick wires,

(b) an increase of the absolute upper limit of efficiency achievable with fine grids,

(c) frequency-selective performance in either broad (in transmission) or narrow (in reflection) frequency bands, and

(d) a possibility of tuning the operation bands by varying the device inter-layer spacing or tilting the polarizer with respect to the incident wave.

An optimal design has been proposed for manufacturing and electromagnetic testing of polarizers with account of possible imperfections and manufacturing tolerances. A few sets of polarizer-analyzer pairs of dual-layer grid polarizers of the aperture diameter D=90mm and D=170mm have been fabricated for electromagnetic testing in the lower frequency band of 75-110 GHz and, at the later stage, in the high frequency band of 100-300 GHz.

Electromagnetic testing of dual-layer grid polarizers has been carried out in the frequency band of 75-110 GHz by using the VNA test facility. Experimental data are shown to be in a good agreement with theoretical predictions.

A steel-wire dual-grid polarizer of a robust design (of the wire thickness w=0.08mm and grid period p=0.27mm) shows the polarization extinction ratio of –65 dB to –55 dB in the frequency band of f = 75-110 GHz in transmission and about –60 dB at the “spike” frequency f = 95 GHz in reflection (at the beam incidence angle of 20 degrees, where both the “spike” frequency and the relevant incidence angle are defined by the grid interlayer spacing).

Thus, dual-layer polarizers of this kind, while having a very robust design, show an excellent performance that coincides with theoretical predictions and, when using slightly finer grids (e.g., of w=0.02mm and p=0.10mm), are capable to operate with equally high efficiency in the relevant bands up to the terahertz frequencies.

8. References

[1] G. R. Bird and M. Parrish, "The wire grid as a near-infrared polarizer," *J. Opt. Soc. Am.*, vol. 50, no. 9, pp. 875–891 (1960)

[2] J. J. Wang *et al.*, "Innovative high-performance nanowire-grid polarizers and integrated isolators," *IEEE J. Select. Topics Quantum Electron.*, Vol. 11, No. 1, 241–253 (2005)

[3] A. D. Turner, J. J. Bock, J. W. Beeman *et al.*, "Silicon nitride micromesh bolometer array for submillimeter astrophysics," *Appl. Optics*, vol. 40, no. 28, pp. 4921–4932 (2001)

[4] T. Manabe and A. Murk, "Transmission and reflection characteristics of slightly irregular wire-grids with finite conductivity for arbitrary angles of incidence and grid rotation, *IEEE Trans. Antennas and Propagat.,* Vol. 53, No. 1, pp. 250-259 (2005)

[5] T. Manabe *et al*, "A new configuration of polarization-rotating dual-beam interferometer for space use," *IEEE Trans. Microwave Theory Tech*., Vol. 51, No. 6, pp. 1696-1704 (2003)

[6] P. C. Deguzman and G. P. Nordin, "Stacked subwavelength gratings as circular polarization filters," *Appl. Optics*, Vol. 40, No. 31, pp. 5731–5737 (2001)

[7] A. V. Arzhannikov and S. A. Kuznetsov, "Multigrid interference structures with variable selective characteristics," in *Digest 2004 Joint 29th Int. Conf. on Infrared and Millimeter Waves and 12th Int. Conf. on Terahertz Electronics,* Sept. – Oct. 2004, pp. 353–354.

[8] K. Yasumoto, H. Toyama, and T. Kushta, "Accurate analysis of two-dimensional electromagnetic scattering from multilayered periodic arrays of circular cylinders using lattice sums technique", *IEEE Trans. Antennas and Propagat.,* Vol.52, No.10, pp. 2603-2611 (2004)

[9] J. H. W. G. den Boer, G. M. W. Kroesen, W. de Zeeuw and F. J. de Hoog, "Improved polarizer in the infrared: Two wire-grid polarizers in tandem," *Opt. Lett.,* Vol. 20, No. 7, pp. 800–802 (1995).

[10] V. B. Yurchenko and E. V. Yurchenko, "Dual-layer frequency-selective subwavelength-grid polarizers for THz applications," in *Proc. 6th Intl. Kharkov Symposium on Physics and Engineering of Microwaves, Millimeter and Submillimeter Waves and Workshop on Terahertz Technologies (MSMW'07),* Kharkov, Ukraine, June 2007, pp. 222–224.

[11] V. B. Yurchenko and E. V. Yurchenko, “Reciprocity in simulations of bolometric detectors in transmitting mode”, *Int. J. Infrared and Millimeter Waves*, vol.27, no.3, pp.355-371 (2006)

[12] L. A. Wainshtein, “To electrodynamic theory of gratings. Part I, II”, in *Elektronika Bol’shikh Moshchnosrei, Vol.2*, P.L. Kapitsa and L.A. Wainshtein, Eds., Moscow, 1963, pp.26-73 [Engl. transl. in ***High-Power Electronics.*** Oxford: Pergamon, 1966, pp. 14-48].

[13] V. B. Yurchenko and A. Altintas, “Anti-shielding effect of a cylindrical grid of metal wires”, *PIERS'98: Progress in Electromagnetic Research Symposium*, July 13-17, 1998, IRESTE, Nantes, France, vol.3, pp.1120 (1998)

[14] T. L. Zinenko, A. I. Nosich, and Y. Okuno, “Plane wave scattering and absorption by resistive-strip and dielectric-strip periodic gratings”, *IEEE Trans. Antennas and Propagat.,* vol.46, no.10, pp.1498-1505 (1998)

[15] V. B. Yurchenko, A. Altintas, and A. I. Nosich, "Numerical optimization of a cylindrical reflector-in-radome antenna system", *IEEE Trans. Antennas and Propagat.,* vol.47, no.4, pp.668-673 (1999)

[16] V. B. Yurchenko, "Analytical regularization technique for electromagnetic wave scattering from anisotropic and composite screens", in *Proc. 24th Antenna Symposium*, M. R. Rayner, Ed., London, UK, 18 April 2000, pp.42-45 (2000)

[17] A. F. Krupnov et al., “Ultra-low absorption measurement in dielectrics in millimeter- and submillimeter-wave range,” *IEEE Trans. Microwave Theory Tech*., Vol. 47, No. 3, pp. 284–289 (1999)

[18] V. B. Yurchenko and E. V. Yurchenko, “Enhanced Dual-Layer Grid Polarizers for THz Application”, in *Proc. 5th Intl. Workshop on Electromagnetic Wave Scattering (EWS’2008),* 22-25 October, 2008, Antalya, Turkey, pp. 1-1 – 1-6.

[19] V. B. Yurchenko, J. A. Murphy, J. Barton, J. Verheggen, and K. Rodgers, “Dual-Layer Frequency-Selective Grid Polarizers on Thin-Film Substrates for THz Applications”, in *Proc. EuMW 2008: 38th European Microwave Conference 2008 (EuMC-2008),* 28-31 October, 2008, Amsterdam, The Netherlands, pp. 10-14 – 10-17.

9. List of Symbols, Abbreviations, and Acronyms

$E_{x,y}^{+\delta}$, $E_{x,y}^{-\delta}$ are the electric field x and y components chosen at the (+) right-hand and (-) left-hand sides of grid, respectively, in the effective boundary conditions (5.1)

$H_{x,y}^{+\delta}$, $H_{x,y}^{-\delta}$ are the electric field x and y components chosen at the (+) right-hand and (-) left-hand side of grid, respectively, in the effective boundary conditions (5.1)

$R_{X,Y}$, $S_{X,Y}$ are the relevant coefficients in the effective boundary conditions (5.1), i.e., the effective electric sheet resistance and the magnetic sheet conductance x and y components, respectively

δ is the distance from the grid where the average values of both the electric and magnetic fields are chosen in the effective boundary conditions (5.1) ($p < \delta << d \sim \lambda$)

p is the grid period

w is the wire thickness in the wire grids and microstrip width in microstrip gratings

s is the grid slot size ($p = w + s$)

d is the inter-layer spacing in the dual-layer polarizer

σ is the electric conductivity of the wire (microstrip) material

θ is the angle between the wave propagation direction and the normal to the polarizer plane

λ is the radiation wavelength

f is the radiation frequency

f_n is the value of the "spike" frequency of order n observed in the polarization extinction ratio spectral curves in reflection

D is the grid aperture diameter

D_M is the open resonator mirror diameter

R_M is the open resonator mirror curvature radius

L_M is the distance between the open resonator mirrors

w_0 is the Gaussian beam half-width at the beam waist position

w_M is the Gaussian beam half-width at the open resonator mirror position

Q is the quality factor of the open resonator

S_{11}, S_{12} are the scattering matrix coefficients of the polarizer to be measured as functions of frequency at various polarizations of incident waves

$R_{RE} = E_R / H_R$ is the ratio of reflected amplitudes measured for the incident E- (co-) and H- (cross-) polarized waves (when either E or H field is parallel to grid wires)

$R_{TR} = H_T / E_T$ is the ratio of transmitted amplitudes measured for the incident H- (cross-) and E- (co-) polarized waves (when either H or E field is parallel to grid wires)

$R_E = E_R / E_T$ is the polarization extinction ratio defined by relating reflected and transmitted wave amplitudes of the same incident polarization (E-polarization case)

$R_H = H_T / H_R$ is the polarization extinction ratio defined by relating reflected and transmitted wave amplitudes of the same incident polarization (H-polarization case)

Acknowledgement of Sponsorship: Effort sponsored by the Air Force Office of Scientific Research, Air Force Material Command, USAF, under grant number FA8655-08-1-3049. The U.S. Government is authorized to reproduce and distribute reprints for Government purpose notwithstanding any copyright notation thereon.

Disclaimer: The views and conclusions contained herein are those of the author and should not be interpreted as necessarily representing the official policies or endorsements, either expressed or implied, of the Air Force Office of Scientific Research or the U.S. Government.

Disclosure of Inventions: I certify that there were no subject inventions to declare during the performance of this grant.